Critical Properties and Vapor-Liquid Equilibria of the Binary System Propane + Neopentane

Douglas W. Hissong† and Webster B. Kay

Department of Chemical Engineering, The Ohio State University, Columbus, Ohio 43210

James C. Rainwater*

Thermophysics Division, National Institute of Standards and Technology, Boulder, Colorado 80303

Vapor-liquid equilibrium data extending to critical pressures are reported for five mixtures of propane with neopentane. The data in pressure, temperature, and density are correlated to high accuracy by the Leung-Griffiths model as modified by Moldover, Rainwater, and co-workers. In addition, a complete bibliography of similar experiments on binary mixtures from the laboratory of W.B.K. is presented.

Introduction

Recently, several papers (*1-6*) have appeared which have included hitherto unpublished vapor-liquid equilibrium (VLE) data from the Ohio State University laboratory, together with correlations based on classical equations of state. The experiments described in those papers consisted of measurements of dew-bubble curves in pressure (P), temperature (T), and (in most cases) density (ρ) along isopleths or loci of fixed mole fraction (x) for a selected set of binary mixtures. A large number of dew and bubble points have been measured very near the critical locus of each mixture, so the critical regions have been very well characterized.

In this paper and the following one (*7*) we present some additional, hitherto unpublished VLE data from the Ohio State laboratory. Furthermore, we correlate these measurements by a relatively new thermodynamic technique, the Leung-Griffiths model (*8*) as modified by Moldover, Gallagher, and Rainwater (*9-13*), which is specifically designed to be accurate within the critical region. This model has been successful in correlating more than 40 binary mixtures (*9-17*) and has consistently led to excellent agreement with the experiments of Kay and co-workers in particular (*14, 16*).

The subject of this first paper is the binary mixture of propane with neopentane (2,2-dimethylpropane or tetramethylmethane) as measured by Hissong (*18*). The following paper (*7*) examines binary mixtures of propane with each of the five isomers of hexane, as measured by Chun (*19*). When combined with correlations of the propane + *n*-pentane mixture (*13, 20, 21*), and of the propane + isopentane mixture (*14, 22*), accurate data and correlations are now available for all mixtures of propane with alkanes of five or six carbon atoms.

Table I summarizes the VLE experiments of Kay and co-workers that are amenable to correlation with the modified Leung-Griffiths theory. As a general policy, before 1980 smoothed data (at even intervals of pressure) were presented in archival journals, whereas original or raw data were preserved in theses and, in most cases, made available through an auxiliary publication serivce. The unpublished industrial reports and M.Sc. theses cited in Table I are only available from the respective institutions, but J.C.R. is developing a comprehensive database with original data from these sources and from other laboratories, and can provide data files or tables upon request.

The table excludes studies of binary mixtures such as benzene + water (*73*) and helium + *n*-butane (*74*) which have discontinuous critical loci and therefore cannot be correlated by the modified Leung-Griffiths model. Also excluded, for the most part, are a large number of studies in which dew and bubble points (usually without densities) were measured only very close to the critical locus; several such papers have already been cited (*4, 6, 69*). The primary objective of this second class of experiments was to determine the critical locus rather than the coexistence surface. In all of the experiments cited in Table I, the fluids were subjected to a degassing process in which dissolved air was carefully removed, as described below. However, for the second class of experiments, the fluids in some cases were not degassed.

In a series of three papers, Kay and Hissong (*75-77*) have presented graphically data from the second class of experiments for 50 hydrocarbon mixtures. Original data are tabulated in the theses cited therein, except for those from the thesis of Hissong (*78*) which are only available in graphical form. Similar papers, with original data available from the theses cited therein, are by Kay (*70*) on acetone + *n*-alkane mixtures, by Kreglewski and Kay (*51*), and by Mousa *et al.* (*79*). Pak and Kay (*80*) have reported direct critical locus measurements on 15 additional hydrocarbon mixtures. Finally, in the study of carbon dioxide + benzene and sulfur dioxide + benzene by Kay and Kreglewski (*81*), the critical loci were measured directly but the dew and bubble curves reported there were inferred from an equation of state rather than measured.

Propane + neopentane is one of a relatively few number of neopentane mixtures for which data on phase equilibrium are available in the critical region. VLE data that span the full phase diagram have been presented for mixtures of neopentane with carbon dioxide (*82, 83*) and tetramethylsilane (*84*). More limited studies provide VLE along critical isotherms for mixtures of neopentane with methane (*85, 86*), argon (*85, 87*), hydrogen sulfide (*88*), and carbon tetrafluoride (*89*), and along isopleths for mixtures of neopentane with *n*-pentane and cyclopentane (*90*). In addition, critical temperature loci have been measured for mixtures of neopentane with *n*-pentane, *n*-hexane, cyclohexane, benzene, and toluene (*91*).

While the modified Leung-Griffiths model does show promise for correlating limited VLE data (*15*), it is best applied

† Present address: Exxon Production Research Corp., P.O Box 2189, Houston, TX 77001.

0021-9568/93/1738-0486$04.00/0

Table I. VLE Bibliography of Kay and Co-workers

	mixture	reference: original data	reference: smoothed data	reference: critical locus	number of isopleths
1	ethane + *n*-heptane	23	24	24	5
2	ethane + *n*-butane	25	26	26	5
3	*n*-butane + *n*-heptane	27	28	28	5
4	ethylene + *n*-heptane	29	30	30	8
5	ethane + benzene	31	32	32	7
6	propane + hydrogen sulfide[a]	33	34	34	7
7	ethane + hydrogen sulfide[a]	35	36	36	6
8	carbon dioxide + hydrogen sulfide	37	38	38	8
9	methanol + 1-butanol	39	40	40	4
10	diethyl ether + 1-butanol	39	40	40	4
11	isobutanol + 1-butanol	39	40	40	3
12	ethane + cyclohexane	41	42	42	6
13	ammonia + *n*-butane[a]	43	44[b]	44	6
14	ammonia + isooctane[a] (2,2,4-trimethylpentane)	45[c]	46	46	11
15	methanol + benzene	47	48	48	5
16	ethanol + benzene	47	48	48	7
17	1-propanol + benzene	47	48	48	7
18	1-butanol + benzene	47	48	48	6
19	propane + *n*-butane	49	50	51, 50	5
20	propane + *n*-pentane	52	50	51, 50	5
21	propane + *n*-hexane	53	54	51, 54	6
	propane + *n*-hexane	7, 19		7, 55	5
22	propane + 2-methylpentane	7, 19		7, 55	5
23	propane + 3-methylpentane	7, 19		7, 55	5
24	propane + 2,2-dimethylbutane	7, 19		7, 55	5
25	propane + 2,3-dimethylbutane	7, 19		7, 55	5
26	propane + *n*-heptane[d]	56	54	51, 54	5
27	propane + *n*-octane	57	58	51, 58	6
28	*n*-butane + *n*-octane	59	58	58	5
29	*n*-butane + *n*-pentane	60	61	61	5
30	*n*-butane + *n*-hexane	62	61	61	6
31	(perfluoromethyl)cyclohexane (PFMCH) + *n*-hexane[a]	63, 1		64	5
32	PFMCH + 2-methylpentane[a]	63, 1		64	6
33	PFMCH + 3-methylpentane[a]	63, 1		64	6
34	PFMCH + 2,2-dimethylbutane[a]	63, 1		64	6
35	PFMCH + 2,3-dimethylbutane[a]	63, 1		64	6
36	perfluorocyclobutane + *n*-propane[a]	65, 2		66	7
37	pentane + pent-1-ene[f]	67, 3		67, 3	3
38	acetone + *n*-pentane[a]	68, 5		5	5
	acetone + *n*-pentane[a]	69,[d,e] 5		70	5
39	propane + neopentane	18[g]		18[g]	5
40	ethane + perfluoro-*n*-heptane	71[h]		72	5
41	propane + perfluoro-*n*-heptane	71[h]		72	6
42	*n*-butane + perfluoro-*n*-heptane[a]	71		72	6
43	*n*-pentane-perfluoro-*n*-heptane[a]	71		72	6
44	*n*-hexane + perfluoro-*n*-heptane[a]	71		72	7
45	*n*-heptane + perfluoro-*n*-heptane[a]	71		72	10
46	*n*-octane + perfluoro-*n*-heptane	71[e]		72	8
47	*n*-nonane + perfluoro-*n*-heptane	71[h]		72	6

[a] Azeotropic mixtures. [b] Smoothed in composition as well as pressure. [c] Also contains liquid–liquid equilibrium data. [d] coexisting density data absent. [e] Liquid and vapor data all very close to critical locus. [f] Coexisting liquid density data absent. [g] This paper. [h] Liquid data all very close to critical locus.

to experiments such as those listed in Table I with coexisting density data and dew–bubble curves over a wide range of pressures. As seen from Table I, with the publication of this paper and the following one, data from all of the more thorough studies of Kay and co-workers are now available in the archival literature, except for those of Jordan (*71*). Attempts to correlate Jordan's data with the modified Leung–Griffiths model are currently in progress; these efforts are complicated by the presence of azeotropy and some peculiar features of hydrocarbon + fluorocarbon mixtures. A similar publication based on Jordan's data is planned, pending some further analysis.

Apparatus and Experimental Data

The apparatus used in this work was, for the most part, identical to that described by Kay and Rambosek (*34*). Figure 1 presents a schematic diagram of this apparatus, each component of which will be referred to in the following.

The hydrocarbon sample was confined over mercury in a thick-walled glass capillary tube (a) of approximately 3-mm bore, which was mounted in a compressor block (b) and surrounded by a vacuum-insulated heating jacket (c). The temperature was maintained by boiling a pure organic compound in the side arm flask (d) connected to the bottom of the jacket. A stream of air was blown across the jacket near its top (e) to condense the vapors of the boiling compound. The top of the heating jacket was connected through a water condenser (f) to a mercury manometer (g) and a series of large containers (h) which provided a surge volume of about 0.057 m^3 (57 L). The pressure in this system was controlled by allowing air to pass through two 100-mL bulbs, one of which was connected to a vacuum pump (i) and the other was open to the atmosphere (j). By varying the boiling pressure within the jacket in this manner, we could control the sample temperature very precisely.

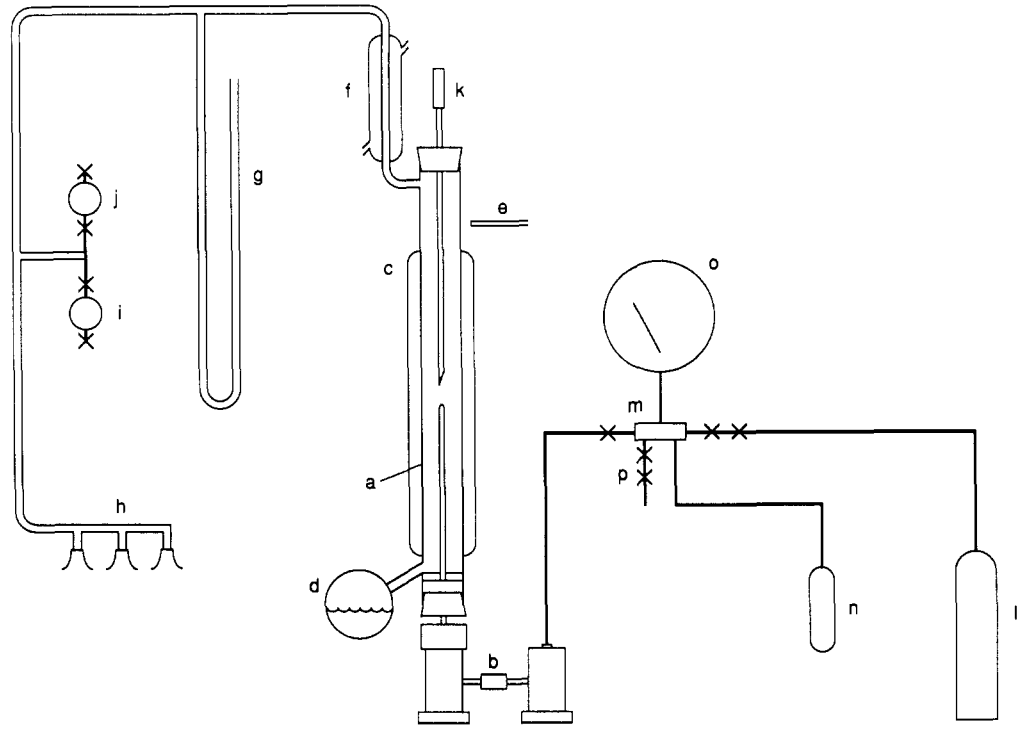

Figure 1. Apparatus to measure phase equilibrium in pressure, volume, and temperature.

The sample temperature was measured with a copper–constantan thermocouple (k), which was inserted into the top of the heating jacket. The tip of the thermocouple was about 1 cm above the closed end of the sample tube, and the cold junction was kept in a Dewar flask containing an ice–water mixture. The thermocouple emf was measured with a precision potentiometer. The thermocouple was calibrated by comparing it with a platinum resistance thermometer, which had been certified by the National Bureau of Standards.

Pressure was transmitted to the sample through mercury in the U-shaped compressor block. Compressed nitrogen from a cylinder (l) entered a manifold (m) to which were connected a 1-L surge tank (n) and a precision Bourdon gauge (o), which was calibrated by comparison with a dead weight gauge. The manifold was connected to the back leg of the compressor block. Through the double valve systems on the high-pressure nitrogen inlet and the exhaust line (p) of the manifold, small quantities of nitrogen could be added to, or removed from, the system. In this way, the pressure of the sample could be precisely controlled.

The sample volume was measured by determining the position of the interface in the capillary tube with a precision cathetometer. The volume of the tube was known as a function of the distance from the closed end by a previous calibration. Several mercury levels were also measured for use in calculating the sample pressure. The sample in the capillary tube was stirred by moving a steel ball within the tube by means of a strong magnet held outside the heating jacket.

The propane and neopentane used in this work were high-purity research-grade materials. They were degassed (freed of dissolved air) by a cyclic operation which involved freezing, pumping off released gas, melting, and distillation at low pressure. They were then sealed into glass ampules. The experimental tube was filled with mercury while attached to a vacuum train and under high vacuum. The propane and neopentane were charged to the tube by mercury displacement. The critical properties of both pure components were measured and compared with published values as a check on the methods used and the purity of the hydrocarbons.

Table II. Critical Properties of Binary Systems of Neopentane (1) + Propane (2)

	T_c (K)		P_c (MPa)		ρ_c (kg/m^3)	
x_2	exptl	fit	exptl	fit	exptl	fit
0.1581	426.46	426.641	3.4798	3.4783	232.8	230.44
0.4573	410.32	410.319	3.9436	3.9461	230.7	228.14
0.6625	396.96	396.960	4.1903	4.1869	230.0	227.26
0.8109	385.88	385.882	4.2855	4.2883	227.7	226.19
0.9339	375.71	375.707	4.2936	4.2923	221.7	223.51

Compositions of the mixtures were determined from measured component volumes and known densities. Details of these procedures have been described by Kay and Rambosek (*34*). The measured pressures were corrected by subtracting the vapor pressure of mercury at the measured temperature. The magnitude of the corrections for mercury vapor dissolved in hydrocarbon mixtures has been analyzed by Kay and Pak (*92*); at the temperatures of this study such corrections are very small.

Five mixtures of propane and neopentane were studied. The pressure, temperature, and volume at the bubble and dew points were measured over a temperature range from approximately 350 K to the maximum temperature at which liquid and vapor coexist. The critical point was determined visually as the conditions at which the meniscus between the vapor and liquid phases disappeared. Measured critical points are listed in Table II.

Dew and bubble points for the propane + neopentane mixture are listed in Table III and are displayed in the P–T plot of Figure 2 and the T–ρ plot of Figure 3. Also shown in the figures are the pure-fluid coexistence loci, the critical locus, and the predictions of the modified Leung–Griffiths model as discussed in the following sections. Clearly the data are highly self-consistent, in that they form smooth curves with no evidence of scatter on the scale of the figures. Also, the region close to the critical point has been thoroughly investigated, as is evident from the figures.

The precision of the data is estimated to be as follows: temperature, 0.1 K; pressure, 0.014 MPa (2.0 psi); density, 1.0 kg/m^3 for the liquid and 0.1 kg/m^3 for the vapor. However, in the critical region, the uncertainty in the values reported

Table III. Neopentane (1) + Propane (2) Data

P (MPa)	T (K)	ρ (g/cm^3)	P (MPa)	T (K)	ρ (g/cm^3)
		$x_2 = 0.1581$			
1.1342	357.48	0.497 37	2.2977	404.11	0.076 88
1.2426	362.11	0.491 04	2.6728	407.45	0.390 74
1.3486	366.55	0.482 00	2.4384	407.45	0.083 84
1.4346	370.08	0.475 99	2.7947	410.51	0.379 92
1.5285	373.62	0.470 34	2.5683	410.51	0.091 48
1.6073	376.31	0.465 80	2.9452	413.75	0.367 80
1.6991	379.55	0.458 93	2.7280	413.75	0.100 06
1.7800	382.28	0.452 82	3.0878	417.14	0.353 40
1.8706	385.15	0.448 54	2.8934	417.14	0.111 42
1.6332	385.21	0.049 39	3.2056	419.93	0.335 97
1.8988	386.08	0.446 25	3.0360	419.94	0.123 55
1.6605	386.08	0.050 17	3.3157	422.23	0.319 80
1.9711	388.35	0.441 56	3.1519	422.23	0.136 25
1.7331	388.35	0.053 01	3.3847	423.71	0.306 06
2.1025	392.35	0.431 34	3.2394	423.71	0.147 19
1.8659	392.35	0.058 16	3.4274	424.59	0.294 72
2.2189	395.67	0.423 57	3.3001	424.59	0.155 30
1.9823	395.67	0.063 17	3.4708	425.58	0.276 93
2.3273	398.70	0.415 29	3.3654	425.58	0.167 91
2.0953	398.70	0.067 65	3.4792	426.13	0.257 57
2.4248	401.32	0.409 51	3.4068	426.13	0.179 31
2.1923	401.33	0.071 91	3.4798	426.46	0.232 81
2.5353	404.11	0.400 25			
		$x_2 = 0.4573$			
1.9205	361.27	0.458 07	3.4406	406.16	0.124 65
2.0357	364.67	0.451 30	3.9091	408.03	0.289 97
2.1855	369.06	0.442 58	3.5805	408.07	0.137 39
2.3346	372.98	0.433 45	3.9509	409.51	0.261 99
2.4909	377.13	0.423 91	3.7001	409.52	0.151 42
2.6643	381.14	0.414 13	3.9437	409.08	0.272 14
2.8378	385.13	0.403.86	3.6592	409.09	0.146 17
3.0165	389.11	0.390 70	3.9302	408.75	0.278 01
2.4622	389.10	0.071 70	3.6335	408.76	0.143 44
3.2709	394.76	0.371 52	3.9442	409.29	0.267 21
2.7467	394.76	0.083 80	3.6835	409.32	0.148 71
3.5189	399.82	0.350 27	3.9513	409.79	0.253 18
3.0350	399.83	0.097 98	3.7243	409.81	0.154 75
3.6754	402.97	0.333 10	3.9515	410.05	0.242 91
3.2152	402.97	0.109 45	3.7550	410.06	0.158 99
3.8225	406.16	0.309 63	3.9436	410.32	0.230 73
		$x_2 = 0.6625$			
2.3310	357.47	0.438 13	3.9723	391.27	0.320 16
2.4756	361.00	0.429 57	3.4974	391.28	0.111 85
1.8816	361.04	0.046 65	4.1069	393.93	0.295 89
2.6512	364.95	0.422 12	3.7062	393.94	0.126 65
2.0442	364.96	0.051 56	4.1761	395.74	0.269 58
2.8200	368.68	0.411 33	3.8649	395.76	0.140 75
2.2050	368.72	0.056 64	4.1935	396.17	0.258 33
2.9943	372.34	0.401 23	3.9095	396.18	0.145 82
2.3710	372.37	0.062 18	4.1955	396.43	0.249 84
3.1638	376.00	0.387 68	3.9410	396.44	0.148 94
2.5573	376.00	0.068 66	4.1937	396.73	0.238 41
3.3207	379.04	0.377 92	3.9727	396.75	0.153 40
2.7279	379.05	0.074 72	3.9912	396.92	0.155 69
3.4777	382.09	0.367 34	4.1903	396.96	0.230 02
2.9046	382.11	0.081 67	4.0362	397.37	0.162 77
3.6446	385.18	0.355 30	4.0670	397.56	0.169 18
3.0826	385.19	0.089 81	4.0952	397.68	0.173 71
3.7881	387.85	0.341 30	4.1472	397.83	0.188 59
3.2526	387.86	0.098 33			
		$x_2 = 0.8109$			
2.6508	355.11	0.415 35	4.1291	382.18	0.303 05
2.8571	359.32	0.405 26	3.7950	382.19	0.123 82
2.3619	359.34	0.058 54	4.1602	382.77	0.296 59
2.9892	361.85	0.397 27	3.8519	382.77	0.127 37
2.4924	361.88	0.062 71	4.1983	383.48	0.288 02
3.1421	365.08	0.386 32	3.9102	383.48	0.132 57
2.6683	365.10	0.068 51	4.2306	384.12	0.279 92
3.3018	368.04	0.377 73	3.9620	384.14	0.137 93
2.8362	368.05	0.074 50	4.2536	384.64	0.270 05
3.4657	370.84	0.367 10	4.0127	384.66	0.143 02
3.0058	370.89	0.081 17	4.2708	385.17	0.259.46
3.6090	373.34	0.356 33	4.0654	385.18	0.149 09
3.1527	373.35	0.087 79	4.2780	385.50	0.246 86
3.7554	375.97	0.346 04	4.1003	385.51	0.154 18

Table III (Continued)

P (MPa)	T (K)	ρ (g/cm³)	P (MPa)	T (K)	ρ (g/cm³)
		x_2 = 0.8109			
3.3304	375.97	0.095 83	4.2853	385.66	0.238 18
3.9248	378.76	0.328 93	4.1245	385.68	0.156 74
3.5319	378.77	0.105 97	4.2855	385.88	0.227 67
4.0076	380.14	0.319 58	4.1581	385.95	0.162 45
3.6327	380.16	0.112 36	4.1735	386.18	0.168 15
4.0904	381.46	0.309 92	4.2768	386.20	0.212 76
3.7422	381.48	0.119 28	4.2330	386.45	0.180 81
		x_2 = 0.9339			
3.0041	358.34	0.078 62	4.1268	372.78	0.298 09
3.2026	358.35	0.376 36	4.1622	374.73	0.156 80
3.2058	361.74	0.087 17	4.2543	374.73	0.269 50
3.4090	361.75	0.362 58	4.1988	375.18	0.164 48
3.3795	364.41	0.095 25	4.2722	375.18	0.257 59
3.5753	364.42	0.351 90	4.2319	375.46	0.171 52
3.5603	367.01	0.104 43	4.2927	375.45	0.244 66
3.7457	367.01	0.339 06	4.2531	375.61	0.177 59
3.7878	370.08	0.118 50	4.2654	375.71	0.181 67
3.9472	370.08	0.320 35	4.2936	375.71	0.221 67
3.9935	372.77	0.135 81	4.2871	375.81	0.193 66

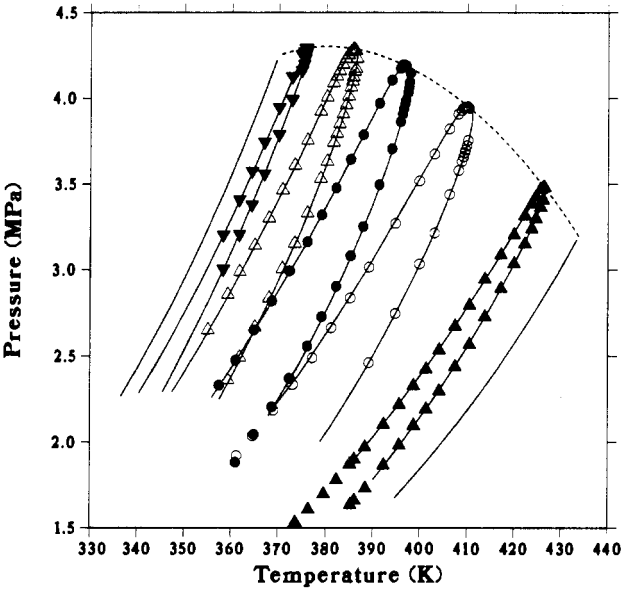

Figure 2. Pressure–temperature phase diagram for the propane + neopentane system. Dew–bubble curves are for the following mole fractions of propane, right to left: 0.1581, 0.4573, 0.6625, 0.8109, 0.9339. The dashed curve is the fitted critical locus, and the solid curves are the results from the modified Leung–Griffiths correlation.

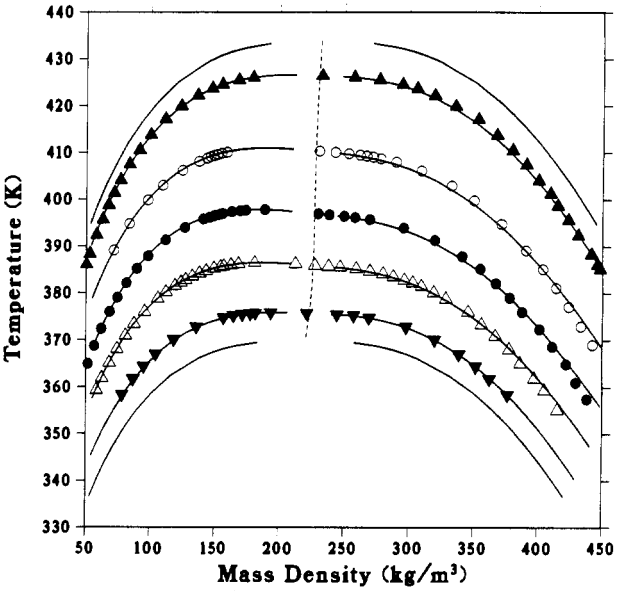

Figure 3. Temperature–density phase diagram for the propane + neopentane system. Compositions are the same as in Figure 2. The dashed curve is the fitted critical locus, the upper and lower solid curves are the coexisting density fits for neopentane and propane, respectively, and the intermediate solid curves are the results from the modified Leung–Griffiths correlation.

may be somewhat greater because of the difficulty of measurements in this region.

Modified Leung–Griffiths Model

The thermodynamic model first proposed by Leung and Griffiths (*8*), and subsequently modified by Moldover, Gallagher, and Rainwater (*9–13*), has proven to be useful in the development of highly accurate VLE correlations of a wide variety of mixtures at high pressures (*9–16*). The model is explained in detail elsewhere (*13*); here we simply summarize the equations needed to perform the calculations.

The basic premise of the model, as put forth by Griffiths and Wheeler (*93*), is that the thermodynamic behavior of mixtures is simpler and more like that of pure fluids if expressed only in terms of field variables. By definition, field variables such as P, T, and the chemical potentials μ_1 and μ_2 of fluids 1 and 2 have the same values in coexisting liquid and vapor phases, whereas "density variables" such as x have differing values. Functions of field variables are, of course, also field variables.

The independent field variables of the model are

$$\zeta = \frac{e^{\mu_1/RT}}{Ke^{\mu_2/RT} + e^{\mu_1/RT}} \quad (1)$$

and

$$t = \frac{T - T_c(\zeta)}{T_c(\zeta)} \quad (2)$$

where $T_c(\zeta)$ is the mixture critical temperature, R is the gas constant, and K can be a constant or a temperature-dependent function. Since $\mu_1 \to -\infty$ for pure fluid 2 (here propane), and vice versa, $\zeta = 0$ when $x = 1$ and $\zeta = 1$ when $x = 0$. Furthermore, it has been shown (*13*) that if T_c is monotonic in x, which is true for mixtures of propane with neopentane and with the hexane isomers, then a function $K(T)$ exists such that $x = 1 - \zeta$ exactly on the critical line. Then there is a unique T_c for each ζ, $0 \le \zeta \le 1$, and eq 2 serves as a definition of t (a

dimensionless distance from the critical locus) in terms of $T_c(\zeta)$.

According to the model, molar densities along loci of constant ζ on the coexistence surface are given by

$$\rho = \rho_c(\zeta)[1 \pm C_1(\zeta)(-t)^{0.355} + C_2(\zeta)t] \quad (3)$$

where the plus is used for the liquid and the minus is used for the vapor. In P–T space, loci of constant ζ are represented as

$$\frac{P}{T} = \frac{P_c(\zeta)}{T_c(\zeta)}[1 + C_3(\zeta)(-t)^{1.9} + C_4(\zeta)t + C_5(\zeta)t^2 + C_6(\zeta)t^3] \quad (4)$$

For $\zeta = 0$ or 1, the above equations represent fits to the coexisting density curve and the vapor pressure curve of propane or neopentane, respectively. We define $C_i^{(1)} = C_i(\zeta=1)$ and $C_i^{(2)} = C_i(\zeta=0)$, the coefficients of fits to the pure fluid properties. These coefficients are listed in Table IV for propane and neopentane. In previous work (*14*) an earlier fit (*10*) to the propane coexistence data of Clegg and Rowlinson (*94*) was utilized, but it was subsequently found that their liquid densities were significantly lower than those measured in several other independent experiments (*95*). Accordingly, for propane eqs 3 and 4, with $\zeta = 0$, have been refitted to the correlation of Goodwin and Haynes (*95*). The coefficients for neopentane are based on a fit to the correlation of Das *et al.* (*96*).

The coexisting mole fractions are calculated according to the relation

$$x = 1 - \zeta\left\{1 - \zeta\left[\frac{\bar{Q}(\zeta,t)}{\rho} - \frac{\bar{Q}(\zeta,t=0)}{\rho_c(\zeta)} - \bar{H}(\zeta,t)\right]\right\} \quad (5)$$

where use of the liquid or vapor density from eq 3 yields the liquid or vapor composition, respectively, and where

$$\bar{Q}(\zeta,t) = \frac{PT_c(\zeta)}{RTP_c(\zeta)}\frac{d}{d\zeta}\left[\frac{P_c(\zeta)}{T_c(\zeta)}\right] + \frac{P_c(\zeta)}{RT_c(\zeta)}\{C_3(\zeta)(-t)^{1.9} + C_4(\zeta)t + C_5(\zeta)t^2 + C_6(\zeta)t^3\} + \frac{P_c(\zeta)}{R}\frac{d}{d\zeta}\left[\frac{1}{T_c(\zeta)}\right](1+t)[-1.9C_3(\zeta)(-t)^{0.9} + C_4(\zeta) + 2C_5(\zeta)t + 3C_6(\zeta)t^2] \quad (6)$$

and

$$\bar{H}(\zeta,t) = \frac{1}{T_c(x)}\frac{dT_c(x)}{dx}C_H(1 + C_Z\zeta)t \quad (7)$$

Equation 7 introduces two adjustable parameters, C_H and C_Z. The ζ dependence of C_i in eq 4 is given by simple linear interpolation between the pure fluids,

$$C_i(\zeta) = C_i^{(2)} + \zeta[C_i^{(1)} - C_i^{(2)}], \quad i = 3\text{–}6 \quad (8)$$

whereas the functions of eq 3 are given by the slightly more involved expressions

$$C_1(\zeta) = \frac{C_1^{(2)} + \zeta[C_1^{(1)} - C_1^{(2)}]}{1 + C_X(1 + C_Y\zeta)\zeta(1-\zeta)|\bar{Q}(\zeta,0)|/\rho_c(\zeta)} \quad (9)$$

$$C_2(\zeta) = C_2^{(2)} + \zeta[C_2^{(1)} - C_2^{(2)}] + C_R\zeta(1-\zeta) \quad (10)$$

which introduce three more adjustable parameters, C_X, C_Y, and C_R.

Table IV. Model Parameters for Pure Fluids

	neopentane	propane		neopentane	propane
T_c (K)	433.75	369.85	C_3	30.0	29.57
P_c (MPa)	3.196	4.247	C_4	5.902	5.800
ρ_c (kmol/m^3)	3.215	5.001	C_5	−24.99	−24.08
C_1	1.987	1.958	C_6	0.0	1.024
C_2	−0.83	−0.823			

Table V. Parameters of the Critical Locus

T_1 (kmol/(m^3·MPa))	−0.024 979	$\bar{P}_3$ (kmol/m^3)	0.037 995
T_2 (kmol/(m^3·MPa))	0.005 978	$\bar{\rho}_1$ (kmol/m^3)	0.260 078
T_3 (kmol/(m^3·MPa))	−0.000 867	$\bar{\rho}_2$ (kmol/m^3)	−0.271 430
$\bar{P}_1$ (kmol/m^3)	0.470 937	$\bar{\rho}_3$ (kmol/m^3)	0.127 639
$\bar{P}_2$ (kmol/m^3)	0.021 561		

The critical locus is represented by the following expressions as fitted to the experimentally measured mixture critical points (Table II):

$$\frac{1}{RT_c(x)} = \frac{1-x}{RT_{c1}} + \frac{x}{RT_{c2}} + x(1-x)[T_1 + (1-2x)T_2 + (1-2x)^2 T_3] \quad (11)$$

$$x_T = \frac{1/T_{c1} - 1/T_c(x)}{1/T_{c1} - 1/T_{c2}} \quad (12)$$

$$\frac{P_c(x)}{RT_c(x)} = \frac{(1-x_T)P_{c1}}{RT_{c1}} + \frac{x_T P_{c2}}{RT_{c2}} + x_T(1-x_T)[\bar{P}_1 + (1-2x_T)\bar{P}_2 + (1-2x_T)^2\bar{P}_3] \quad (13)$$

$$\rho_c(x) = (1-x_T)\rho_{c1} + x_T\rho_{c2} + x_T(1-x_T)[\bar{\rho}_1 + (1-2x_T)\bar{\rho}_2 + (1-2x_T)^2\bar{\rho}_3] \quad (14)$$

These equations introduce the nine parameters that characterize the critical line, T_i, $\bar{P}_i$, and $\bar{\rho}_i$, i = 1–3. Values of these parameters for the propane + neopentane critical locus are listed in Table V. In some previous correlations (*12*, *16*), the critical locus has been adjusted to optimize the fit to the coexistence surface, thereby causing some disagreement with the mixture critical points as measured and reported by the experimentalist. This procedure is justified in that measurements near or at a critical point are subject to more experimental uncertainty than those removed from the critical locus. For the case of propane + neopentane, a linear least-squares fit to the experimentally measured critical locus yielded an optimal correlation of $T_c(x)$ and $P_c(x)$, but a minor adjustment was needed for $\rho_c(x)$.

Table II compares the experimental critical loci to those obtained from the fits of eqs 11–14. The fits reproduce $T_c(x)$ to within experimental uncertainty and $P_c(x)$ to within 0.08%, while the optimized fit of $\rho_c(x)$ is within 1.2% of the experimental values. A diagram of the experimental and fitted critical pressure as a function of composition is given in Figure 4.

The model just described includes, in addition to parameters for the pure fluid coexistence properties and the critical locus, five parameters to characterize the mixture. However, depending on the complexity of the mixture, not all parameters are always needed. A good measure of the complexity of the mixture or overall width of the dew–bubble curves is (*12*, *13*)

$$\alpha_{2m} = \max[\delta x/(\delta\rho/\rho_c)] \quad (15)$$

where δx and $\delta\rho$ are the changes in x and ρ across the phase boundary in the limit of approach to the critical point. On the basis of studies of a large number of binary mixtures, we have developed the guidelines for nonpolar fluid mixtures

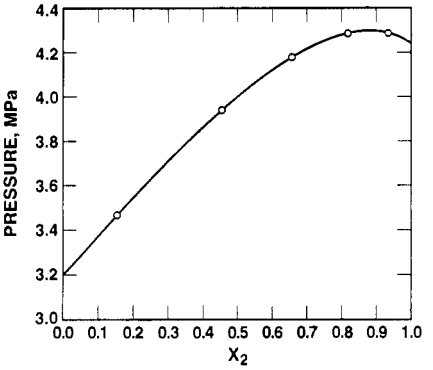

Figure 4. Critical pressure locus for propane + neopentane. The solid curve is the fit according to eqs 12 and 13, and the circles are experimental points.

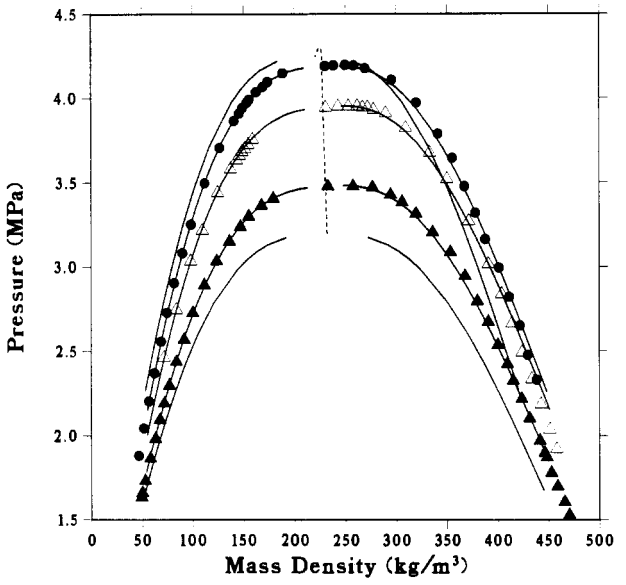

Figure 5. Pressure–density phase diagram for the propane + neopentane system, for the following mole fractions of propane: (●) 0.6625, (△) 0.4573, (▲) 0.1581. The dashed curve is the fitted critical locus. The solid curves are the fitted pure fluid coexistence curves and the results from the modified Leung–Griffiths correlation.

that only C_H is needed if $\alpha_{2m} < 0.1$, C_H and C_X are needed if $0.1 < \alpha_{2m} < 0.17$, and C_R, C_Y, and C_Z are also needed if $0.17 < \alpha_{2m} < 0.25$.

Results

Figures 2 and 3 show the dew–bubble curves as calculated from the modified Leung–Griffiths model and the experimental data. The agreement is excellent, within 0.02 MPa in pressure, 0.3 K in temperature amd 8 kg/m^3 in density, with temperature and composition as independent variables, as shown in Figure 3. It is also instructive to examine isopleths on a pressure–density diagram, although because the critical pressure has a maximum, isopleths near that maximum overlap and lead to a cluttered figure. Consequently, in the pressure–density plot of Figure 5, the two dew–bubble curves richest in propane are omitted. With pressure and composition as independent variables, again the densities are correlated to within 8 kg/m^3, with the largest discrepancies at the highest liquid densities. For these three isopleths, the maxima (maxcondentherm points) in Figure 3 are on the vapor sides, whereas the maxima (maxcondenbar points) in Figure 5 are on the liquid sides.

For this mixture, $\alpha_{2m} = 0.104$. As expected for mixtures in the range $0.1 \leq \alpha_{2m} \leq 0.17$, nonzero values for only two of the five adjustable parameters in eqs 7, 9, and 10 are needed; in particular $C_H = -7$ and $C_X = 0.25$ for propane + neopentane.

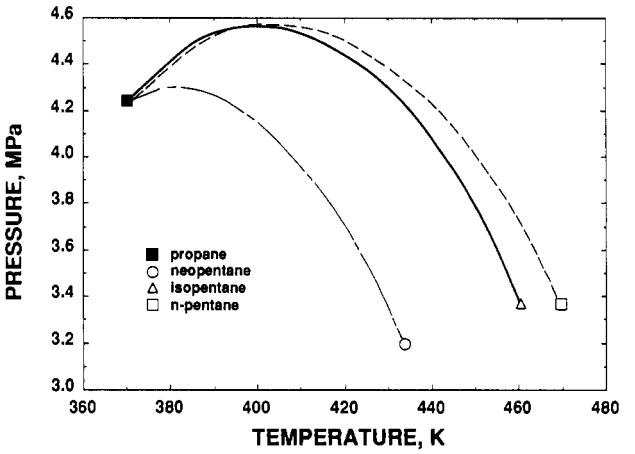

Figure 6. Fitted critical loci for the mixtures propane + neopentane (*18*), broken line; propane + isopentane (*22*), solid line; and propane + *n*-pentane (*50*), dashed line.

Rainwater and Williamson (*14*) have similarly correlated the VLE data for propane + isopentane of Vaughan and Collins (*22*), $\alpha_{2m} = 0.137$, $C_H = -6$, $C_X = 0.1$, and Rainwater (*13*) has correlated the VLE data for propane + *n*-pentane of Kay and Oxley (*50*, *52*), $\alpha_{2m} = 0.141$, $C_H = -8$, and $C_X = 0.3$. The latter correlation is in fair agreement with the data of Sage and Lacey (*20*) and in good agreement with the data of Vejrosta and Wichterle (*21*).

Figure 6 shows the critical loci of the mixtures of propane with the three pentane isomers. The maximum critical pressures are 4.302 MPa for the neopentane mixture and 4.575 MPa for both the isopentane mixture and the *n*-pentane mixture. The isopentane mixture data of Vaughan and Collins are rather sparse compared with those of the other two mixtures, so there may be some uncertainty in the parameters for that system. Nevertheless, while each of the propane + pentane mixtures requires only C_H and C_X, there is no obvious trend in the Leung–Griffiths parameters for these mixture correlations.

Acknowledgment

The authors thank John Lynch and Daniel Friend for assistance with the computer graphics.

Literature Cited

(1) Genco, J. M.; Teja, A. S.; Kay, W. B. *J. Chem. Eng. Data* **1980**, *25*, 355.
(2) Barber, J. R.; Kay, W. B.; Teja, A. S. *AIChE J.* **1982**, *28*, 138.
(3) Wolfe, D.; Kay, W. B.; Teja, A. S. *J. Chem. Eng. Data* **1983**, *28*, 319.
(4) Mandlekar, A. V.; Kay, W. B.; Smith, R. L.; Teja, A. S. *Fluid Phase Equilib.* **1985**, *23*, 79.
(5) Hajjar, R. F.; Cherry, R. H.; Kay, W. B. *Fluid Phase Equilib.* **1986**, *25*, 137.
(6) Abara, J. A.; Jennings, D. W.; Kay, W. B.; Teja, A. S. *J. Chem. Eng. Data* **1988**, *33*, 242.
(7) Chun, S. W.; Kay, W. B.; Rainwater, J. C. *J. Chem. Eng. Data*, following paper in this issue.
(8) Leung, S. S.; Griffiths, R. B. *Phys. Rev. A.* **1973**, *8*, 2670.
(9) Moldover, M. R.; Gallagher, J. S. *ACS Symp. Ser.* **1977**, *60*, 498.
(10) Moldover, M. R.; Gallagher, J. S. *AIChE J.* **1978**, *24*, 267.
(11) Rainwater, J. C.; Moldover, M. R. *Chemical Engineering at Supercritical Fluid Conditions*; Ann Arbor Science: Ann Arbor, MI, 1983; p 199.
(12) Moldover, M. R.; Rainwater, J. C. *J. Chem. Phys.* **1988**, *88*, 7772.
(13) Rainwater, J. C. *Supercritical Fluid Technology*; CRC Press: Boca Raton, FL, 1991; p 57.
(14) Rainwater, J. C.; Williamson, F. R. *Int. J. Thermophys.* **1986**, *7*, 65.
(15) Rainwater, J. C.; Jacobsen, R. T. *Cryogenics* **1988**, *28*, 22.
(16) Rainwater, J. C.; Lynch, J. J. *Fluid Phase Equilib.* **1989**, *52*, 91.
(17) Niesen, V. G.; Rainwater, J. C. *J. Chem. Thermodyn.* **1990**, *22*, 777.
(18) Hissong, D. W. M.Sc. Thesis, Ohio State University, 1965.
(19) Chun, S. W. Ph.D. Thesis, Ohio State University, 1964.
(20) Sage, B. H.; Lacey, W. N. *Ind. Eng. Chem.* **1940**, *32*, 992.

(21) Vejrosta, J.; Wichterle, I. *Collect. Czech. Chem. Commun.* **1974**, *39*, 1246.
(22) Vaughan, W. E.; Collins, F. C. *Ind. Eng. Chem.* **1942**, *34*, 885.
(23) Kay, W. B. Liquid-Vapor Phase Equilibrium Relations in the Ethane-n-Heptane Systems. Conference Report; Standard Oil: IN, Mar 11, 1937.
(24) Kay, W. B. *Ind. Eng. Chem.* **1938**, *30*, 459.
(25) Kay, W. B. Liquid-Vapor Equilibrium Composition Relations in Binary Systems of Mixtures II. Ethane-n-Butane System. Conference Report; Standard Oil: IN, Oct 25, 1938.
(26) Kay, W. B. *Ind. Eng. Chem.* **1940**, *32*, 353.
(27) Kay, W. B. Report No. C40-25; Standard Oil: IN, Sept 3, 1940.
(28) Kay, W. B. *Ind. Eng. Chem.* **1941**, *33*, 590.
(29) Kay, W. B. Report No. F45-12; Standard Oil: IN, Aug 22, 1945.
(30) Kay, W. B. *Ind. Eng. Chem.* **1948**, *40*, 1459.
(31) Nevens, T. D. Ph.D. Thesis, Ohio State University, 1950.
(32) Kay, W. B.; Nevens, T. D. *Chem. Eng. Prog. Symp. Ser.* **1952**, *48* (3), 108.
(33) Rambosek, G. M. Ph.D. Thesis, Ohio State University, 1950.
(34) Kay, W. B.; Rambosek, G. M. *Ind. Eng. Chem.* **1953**, *45*, 221.
(35) Brice, D. B. Ph.D. Thesis, Ohio State University, 1950.
(36) Kay, W. B.; Brice, D. B. *Ind. Eng. Chem.* **1953**, *45*, 615.
(37) Bierlein, J. A. Ph.D. Thesis, Ohio State University, 1951.
(38) Bierlein, J. A.; Kay, W. B. *Ind. Eng. Chem.* **1953**, *45*, 618.
(39) Donham, W. E. Ph.D. Thesis, Ohio State University, 1953.
(40) Kay, W. B.; Donham, W. E. *Chem. Eng. Sci.* **1955**, *4*, 1.
(41) Albert, R. E. Ph.D. Thesis, Ohio State University, 1950.
(42) Kay, W. B.; Albert, R. E. *Ind. Eng. Chem.* **1956**, *48*, 422.
(43) Fisch, H. A. Ph.D. Thesis, Ohio State University, 1951.
(44) Kay, W. B.; Fisch, H. A. *AIChE J.* **1958**, *4*, 293.
(45) Warzel, F. M. Ph.D. Thesis, Ohio State University, 1951.
(46) Kay, W. B.; Warzel, F. M. *AIChE J.* **1958**, *4*, 296.
(47) Skaates, J. M. Ph.D. Thesis, Ohio State University, 1961.
(48) Skaates, J. M.; Kay, W. B. *Chem. Eng. Sci.* **1964**, *19*, 431.
(49) Barber, J. R. M.Sc. Thesis, Ohio State University, 1964.
(50) Kay, W. B. *J. Chem. Eng. Data* **1970**, *15*, 46.
(51) Kreglewski, A.; Kay, W. B. *J. Phys. Chem.* **1969**, *73*, 3359.
(52) Oxley, J. A. M.Sc. Thesis, Ohio State University, 1962.
(53) Porthouse, J. D. M.Sc. Thesis, Ohio State University, 1962.
(54) Kay, W. B. *J. Chem. Eng. Data* **1970**, *16*, 137.
(55) Chun, S. W.; Kay, W. B.; Teja, A. S. *Ind. Eng. Chem. Fundam.* **1981**, *20*, 278.
(56) Ng, S. M.Sc. Thesis, Ohio State University, 1961.
(57) Genco, J. M. M.Sc. Thesis, Ohio State University, 1962.
(58) Kay, W. B.; Genco, J. M.; Fitchner, D. A. *J. Chem. Eng. Data* **1974**, *19*, 275.
(59) Fitchner, D. A. M.Sc. Thesis, Ohio State University, 1962.
(60) Hoffman, R. L. M.Sc. Thesis, Ohio State University, 1962.
(61) Kay, W. B.; Hoffman, R. L.; Davies, O. *J. Chem. Eng. Data* **1975**, *20*, 333.
(62) Davies, O. L. M.Sc. Thesis, Ohio State University, 1965.
(63) Genco, J. M. Ph.D. Thesis, Ohio State University, 1965.
(64) Genco, J. M.; Teja, A. S.; Kay, W. B. *J. Chem. Eng. Data* **1980**, *25*, 350.
(65) Barber, J. R. Ph.D. Thesis, Ohio State University, 1968.
(66) Barber, J. R.; Kay, W. B.; Teja, A. S. *AIChE J.* **1982**, *28*, 134.
(67) Wolfe, D. B. M.Sc. Thesis, Ohio State University, 1970.
(68) Cherry, R. H. Ph.D. Thesis, Ohio State University, 1966.
(69) Brown, C. H. M.Sc. Thesis, Ohio State University, 1959.
(70) Kay, W. B. *J. Phys. Chem.* **1964**, *68*, 827.
(71) Jordan, L. W. Ph.D. Thesis, Ohio State University, 1959.
(72) Jordan, L. W.; Kay, W. B. *Chem. Eng. Prog. Symp. Ser.* **1963**, *59* (44), 46.
(73) Rebert, C. J.; Kay, W. B. *AIChE J.* **1959**, *5*, 285.
(74) Jones, A. E.; Kay, W. B. *AIChE J.* **1967**, *13*, 717.
(75) Kay, W. B.; Hissong, D. W. *Proc.—Am. Pet. Inst., Div. Refin.* **1967**, *47*, 653.
(76) Hissong, D. W.; Kay, W. B. *Proc.—Am. Pet. Inst., Div. Refin.* **1968**, *48*, 397.
(77) Kay, W. B.; Hissong, D. W. *Proc.—Am. Pet. Inst., Div. Refin.* **1969**, *49*, 13.
(78) Hissong, D. W. Ph.D. Thesis, Ohio State University, 1968.
(79) Mousa, A. E. H. N.; Kay, W. B.; Kreglewski, A. *J. Chem. Thermodyn.* **1972**, *4*, 301.
(80) Pak, S. C.; Kay, W. B. *Ind. Eng. Chem. Fundam.* **1972**, *11*, 255.
(81) Kay, W. B.; Kreglewski, A. *Fluid Phase Equilib.* **1983**, *11*, 251.
(82) Leu, A. D.; Robinson, D. B. *J. Chem. Eng. Data* **1989**, *34*, 315.
(83) Shah, N. N.; Pozo de Fernandez, M. E.; Zollweg, J. A., Streett, W. B. *J. Chem. Eng. Data* **1990**, *35*, 278.
(84) McKinnon, I. R. Ph.D. Thesis, University of Exeter, 1967.
(85) Rogers, B. L.; Prausnitz, J. M. *J. Chem. Thermodyn.* **1971**, *3*, 211.
(86) Prodany, N. W.; Williams, B. *J. Chem. Eng. Data* **1976**, *21*, 55.
(87) Marathe, P.; Sandler, S. I. *J. Chem. Eng. Data* **1991**, *36*, 192.
(88) Leu, A. D.; Robinson, D. B. *J. Chem. Eng. Data* **1992**, *37*, 14.
(89) Reisig, H.; Wisotzki, K. D.; Schneider, G. M. *Fluid Phase Equilib.* **1989**, *51*, 269.
(90) Hill, P. L. Ph.D. Thesis, Ohio State Univ., 1950.
(91) Partington, E. J.; Rowlinson, J. S.; Weston, J. F. *Trans. Faraday Soc.* **1960**, *56*, 479.
(92) Kay, W. B.; Pak, S. C. *J. Chem. Thermodyn.* **1980**, *12*, 673.
(93) Griffiths, R. B.; Wheeler, J. C. *Phys. Rev. A* **1970**, *2*, 1047.
(94) Clegg, H. P.; Rowlinson, J. S. *Trans. Faraday Soc.* **1955**, *51*, 1327.
(95) Goodwin, R. D.; Haynes, W. M. *NBS Monogr. (U.S.)* **1982**, *170*.
(96) Das, T. R.; Reed, C. O.; Eubank, P. T. *J. Chem. Eng. Data* **1977**, *22*, 16.

Received for review October 14, 1992. Revised May 20, 1993. Accepted June 8, 1993. J.C.R. was supported in part by the U.S. Department of Energy, Office of Basic Energy Sciences, Division of Chemical Science.